Splitting probabilities and interfacial territory covered by two-dimensional and three-dimensional surface-mediated diffusion

T. Calandre,[1] O. Bénichou,[1] D. S. Grebenkov,[2] and R. Voituriez[1,3]

[1]*Laboratoire de Physique Théorique de la Matière Condensée (UMR 7600), CNRS/UPMC, 4 Place Jussieu, 75255 Paris Cedex, France*

[2]*Laboratoire de Physique de la Matière Condensée (UMR 7643), CNRS, Ecole Polytechnique, F-91128 Palaiseau Cedex, France*

[3]*Laboratoire Jean Perrin (FRE 3231) CNRS/UPMC, 4 Place Jussieu, 75255 Paris Cedex, France*

(Received 14 October 2013; published 31 January 2014)

We consider the mean territory covered by a particle that performs surface-mediated diffusion inside a spherical confining domain (in two and three dimensions) before exit through an opening on the surface. This quantity can be expressed in terms of the splitting probability between two targets on the surface. We derive a general formula that relates this splitting probability to the mean first passage time to a single target that has been recently calculated for such a surface-mediated diffusion process. This formula is exact for pointlike targets and is shown to be accurate for extended targets. The mean covered territory is then found and analyzed for an arbitrary extension of the exit region in both two- and three-dimensional spherical domains.

DOI: 10.1103/PhysRevE.89.012149 PACS number(s): 05.40.Fb, 82.65.+r

I. INTRODUCTION

Interfacial chemical reactions, involving molecules that react on target sites localized on the boundary of a confining domain [1], have proven to play an important role in various contexts such as reactions in porous media, in vesicular systems [2–4], or in heterogeneous catalysis [5]. At the experimental level, the corresponding trajectories, which combine bulk and surface-mediated diffusion phases, can now be observed at the single molecule scale [6,7]. At the theoretical level, surface-mediated diffusion has raised a growing interest over the past years [8–17]. Such interest is partly due to the possibility of minimizing reaction times by a proper tuning of the desorption rate from the surface, which could constitute a general mechanism of enhancement of reaction kinetics [11,12].

Generally, an important observable that emerges in the context of trapping reactions is the territory covered by a diffusing particle. Interest in this observable, so far essentially studied for standard one-state transport processes (as opposed to surface-mediated diffusion), comes mainly from its relation to the so-called Rosenstock trapping problem, where a particle diffuses in a medium containing a fraction q of immobile randomly distributed reactive sites [18]. The survival probability of the particle after n steps can be written $(1-q)^{S_n}$, where S_n stands for the number of distinct sites visited after n steps. The mean and the leading behavior of the variance of the covered territory S_n have been obtained [18,19], and numerous generalizations have been proposed, including the calculation of the mean number of distinct sites visited by p independent walkers [20] and the determination of the asymptotic behavior of the mean number of distinct sites visited on fractal structures [21,22].

Recently, the question of the interfacial territory covered by a surface-mediated diffusion before exiting a confining domain was raised [23]. The mean of the territory $\mathcal{C}$ covered on the circle by a Brownian particle alternating phases of bulk and surface diffusion before exiting the domain has been calculated. However, this analysis was limited to pointlike exits in two-dimensional (2D) disks. Here, we extend these results in several directions: we first introduce a general formula that relates the splitting probability between two targets on the surface (defined as the probability to reach a given target before the other) to the mean first passage time (MFPT) to a single target (defined as the mean time needed to reach the target for the first time). This formula is exact for pointlike targets and is shown to be accurate for extended targets. Since the MFPT for such surface-mediated diffusion processes has been recently analyzed in depth [11,12,24,25], this approach gives access to explicit expressions of the splitting probabilities. Using this formalism, we next derive analytical results for the mean covered territory (MCT) for an arbitrary extension of the exit in both 2D and three-dimensional (3D) spherical domains.

II. THEORETICAL MODEL

As an archetype of confined interfacial systems, we consider a particle inside a disk (2D) or sphere (3D) $\mathcal{D}$ of radius R (Fig. 1), alternating phases of surface diffusion on the boundary $\partial\mathcal{D}$ with diffusion coefficient D_1 and phases of bulk diffusion inside $\mathcal{D}$ with diffusion coefficient D_2. The time spent during each surface phase is assumed to follow an exponential law with the desorption rate λ, which is characteristic of a first-order kinetics. At each desorption event, the particle is assumed to be radially ejected at a distance a from the surface (otherwise it would be instantaneously readsorbed). Although formulated for any value of this parameter a smaller than R, in most situations of physical interest one has $a \ll R$. We assume that the particle is instantaneously adsorbed on the surface upon encounter; the case of radiative boundary condition used for instance in [17] can be incorporated but is not presented here for the sake of simplicity. In the case of a pointlike exit on a disk (2D), the exact calculation of the splitting probability and the MCT was presented in [23]; we here generalize these results to extended targets on disks (2D) and spheres (3D).

We are interested in the mean territory $\langle\mathcal{C}(\mathbf{r}_S)\rangle$ covered on the boundary $\partial\mathcal{D}$ of the domain by a particle started from S, before exiting through an opening O of angular extension ϵ_O. Note that the opening could also be a reactive site, and is also referred to as target. In the case $3D$, the definition

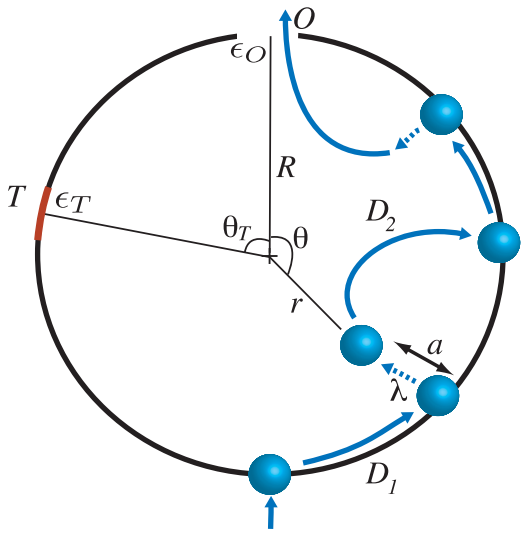

FIG. 1. (Color online) Model of surface-mediated diffusion in a confining domain, with the two targets O and T. Example of crossing trajectory for which the entrance point is opposite to the exit.

of the covered territory requires the introduction of a finite angular particle size ϵ, as in the standard examples of Wiener sausages defined in bulk problems as the territory covered by a spherical Brownian particle of finite size [26]. To compute the MCT, it is useful to reexpress it in terms of so-called splitting probabilities (see [23]) according to

$$\langle \mathcal{C}(\mathbf{r}_S)\rangle = \int_{\partial\mathcal{D}} \Pi(\mathbf{r}_S) d\mathbf{r}_T. \tag{1}$$

Here $\Pi(\mathbf{r}_S)$ is a shortcut notation for the splitting probability $\Pi(\mathbf{r}_O \mid \mathbf{r}_T \mid \mathbf{r}_S)$ to reach the target T of angular extension ϵ_T centered at $\mathbf{r}_T$ on the surface $\partial\mathcal{D}$, starting from the starting point $\mathbf{r}_S$, before exiting the domain through the opening of angular extension ϵ_O centered at $\mathbf{r}_O$ on $\partial\mathcal{D}$. Note that in contrast to the case of a pointlike exit analyzed in [23], the particle can exit the domain during both phases of surface diffusion and bulk diffusion in the case of an extended target, which makes its analyses much more involved.

The splitting probability for surface-mediated diffusion is the central quantity that we analyze in this paper. We consider two typical configurations that are relevant to heterogeneous catalysis: the case of crossing, in which a particle enters the domain from the point opposite to the exit, and the case of return, where a particle enters and exits the domain by the same zone (Fig. 1). In Sec. III, we first analyze the case of pointlike targets in 2D domains and derive an exact relation between the splitting probability with two targets, and the MFPT to a single target. We then show in Sec. IV that this relation yields excellent approximations in the case of extended targets in both two and three dimensions.

III. 2D CASE WITH POINTLIKE TARGETS

In this section, we consider pointlike targets and relate the splitting probability, which involves two targets, to the MFPT, which involves a single target. In the standard polar coordinates, the targets O and T are located at $\mathbf{r}_O = (R,0)$ and $\mathbf{r}_T = (R,\theta_T)$, respectively, while the starting point is $S = (r,\theta)$. The starting point is the classical backward Fokker-Plank equation for the propagator $P(\mathbf{r}',t|\mathbf{r})$ (see [27]), which gives the probability density for the particle started at $t = 0$ at $\mathbf{r}$ to be found at time t at $\mathbf{r}'$. This propagator satisfies

$$\frac{\partial P(\mathbf{r}',t|R,\theta)}{\partial t} = D_1\Delta_1 P(\mathbf{r}',t|R,\theta) + \lambda[P(\mathbf{r}',t|R-a,\theta) - P(\mathbf{r}',t|R,\theta)], \tag{2}$$

$$\frac{\partial P(\mathbf{r}',t|r,\theta)}{\partial t} = D_2\Delta_2 P(\mathbf{r}',t|r,\theta), \tag{3}$$

where $\Delta_1 = \frac{\partial^2}{R^2\partial\theta^2}$ and $\Delta_2 = \frac{\partial^2}{\partial r^2} + \frac{1}{r}\frac{\partial}{\partial r} + \frac{1}{r^2}\frac{\partial^2}{\partial\theta^2}$ are the Laplace operators on the boundary $\partial\mathcal{D}$ and in the interior $\mathcal{D}$ of the disk, acting on the starting point $\mathbf{r} = (R,\theta)$ and $\mathbf{r} = (r,\theta)$, respectively. In Eqs. (2) and (3), the first term on the right-hand side (rhs) stands for the diffusion on the surface and in the bulk, respectively, while the second term on the rhs of Eq. (2) describes desorption events. Following standard methods (see [27,28]), these time dependent equations lead to time independent equations satisfied by the splitting probability:

$$D_1\Delta_1\Pi(R,\theta) + \lambda[\Pi(R-a,\theta) - \Pi(R,\theta)] = 0, \tag{4}$$

$$D_2\Delta_2\Pi(r,\theta) = 0. \tag{5}$$

These equations have to be completed by the boundary conditions

$$\Pi(R,\theta=0) = 0, \quad \Pi(R,\theta=\theta_T) = 1, \tag{6}$$

which come from the very definition of the splitting probability. Note that $\Pi(r,\theta)$ is a continuous function of (r,θ) (even for $r \to R$). An explicit solution of Eqs. (4) and (5) with boundary conditions (6) has been given in [23] without derivation. In Appendix A, we present a detailed derivation of this result for the sake of completeness. Unfortunately, this method does not seem to be applicable for extended targets. For this reason, we introduce another approach for calculating splitting probabilities in terms of MFPTs. This approach relies on the methodology introduced in [29] to analyze first-passage properties of Markovian one-state processes and is extended here to surface-mediated diffusion.

The key ingredient is the pseudo–Green function $H(\mathbf{r}'|\mathbf{r})$ defined by

$$P_{\rm st}(\mathbf{r}') - \delta(\mathbf{r}'-\mathbf{r}) = D_1\Delta_1 H(\mathbf{r}'|R,\theta) + \lambda[H(\mathbf{r}'|R-a,\theta) - H(\mathbf{r}'|R,\theta)], \tag{7}$$

$$P_{\rm st}(\mathbf{r}') - \delta(\mathbf{r}'-\mathbf{r}) = D_2\Delta_2 H(\mathbf{r}'|\mathbf{r}), \tag{8}$$

where $P_{\rm st}(\mathbf{r}')$ is the stationary probability to be at $\mathbf{r}'$ and the Laplace operators Δ_1 and Δ_2 act on the initial state variable $\mathbf{r}$. Note that these equations define $H(\mathbf{r}'|\mathbf{r})$ up to a constant.

First, we express the MFPT to a pointlike target T at $\mathbf{r}_T$ in terms of pseudo–Green functions. Applying standard methods

(see [27,30]) to Eqs. (2) and (3), the MFPT $\langle \mathbf{T}_T\rangle(r,\theta)$ to the target T starting from $\mathbf{r}_S = (r,\theta)$ is shown to satisfy

$$D_1\Delta_1\langle \mathbf{T}_T\rangle(R,\theta) + \lambda[\langle \mathbf{T}_T\rangle(R-a,\theta) - \langle \mathbf{T}_T\rangle(R,\theta)] = -1, \tag{9}$$

$$D_2\Delta_2\langle \mathbf{T}_T\rangle(r,\theta) = -1, \tag{10}$$

$$\langle \mathbf{T}_T\rangle(\mathbf{r}_T) = 0. \tag{11}$$

Direct substitution in Eqs. (9) and (10) yields

$$\langle \mathbf{T}_T\rangle(\mathbf{r}_S) = \frac{1}{P_{\rm st}(\mathbf{r}_T)}(H(\mathbf{r}_T|\mathbf{r}_T) - H(\mathbf{r}_T|\mathbf{r}_S)). \tag{12}$$

The splitting probability to reach the target T before exiting the domain through the opening O can also be expressed in terms of pseudo–Green functions. As in the case of the MFPT, one gets the exact expression for the splitting probability

$$\Pi(\mathbf{r}_S) = \frac{H(\mathbf{r}_T|\mathbf{r}_S) + H(\mathbf{r}_O|\mathbf{r}_O) - H(\mathbf{r}_O|\mathbf{r}_S) - H(\mathbf{r}_T|\mathbf{r}_O)}{H(\mathbf{r}_O|\mathbf{r}_O) + H(\mathbf{r}_T|\mathbf{r}_T) - H(\mathbf{r}_O|\mathbf{r}_T) - H(\mathbf{r}_T|\mathbf{r}_O)}, \tag{13}$$

which can be checked by direct substitution in Eqs. (4) and (5) and using that $P_{\rm st}(\mathbf{r})$ is independent of $\mathbf{r} \in \partial\mathcal{D}$. Finally, combining Eqs. (12) and (13), one finds

$$\Pi(\mathbf{r}_S) = \frac{\langle \mathbf{T}_T\rangle(\mathbf{r}_O) + \langle \mathbf{T}_O\rangle(\mathbf{r}_S) - \langle \mathbf{T}_T\rangle(\mathbf{r}_S)}{\langle \mathbf{T}_T\rangle(\mathbf{r}_O) + \langle \mathbf{T}_O\rangle(\mathbf{r}_T)}. \tag{14}$$

Note that this expression, which plays a key role below, is exact and independent of the domain shape. It can be verified explicitly by using analytical expressions for both the MFPT and the splitting probabilities in the case of circular domains (see below).

IV. EXTENDED TARGETS

In the case of extended targets, Eqs. (12) and (13) are no longer exact. However, we now show that the above approach is still useful and that the relation (14), which is exact for pointlike targets, provides very good approximations in the case of extended targets.

A. Two-dimensional case

We assume here that the target O is defined by the arc $\theta \in [-\epsilon_O,\epsilon_O]$. Note that in the 2D case, the covered territory is well defined even for a particle size $\epsilon = 0$, as opposed to the 3D case discussed below.

To compute $\Pi(\mathbf{r}_S)$ from Eq. (14), one can use either the exact or the approximate expressions of the MFPT to extended targets derived in [12] and summarized in Appendix B.

However, for extended targets, the term $\langle \mathbf{T}_T\rangle(\mathbf{r}_O)$ [resp. $\langle \mathbf{T}_O\rangle(\mathbf{r}_T)$] in Eq. (14) is ambiguous since the starting point *a priori* has to be chosen on the arc $[-\epsilon_O,\epsilon_O]$ of angular extension $2\epsilon_O$ (resp. on the arc $[\theta_T - \epsilon_T,\theta_T + \epsilon_T]$ of angular extension $2\epsilon_T$). To ensure that $\Pi(\mathbf{r}_S)$ vanishes on the boundary of the target O [$\Pi(R,\pm\epsilon_O) = 0$], and satisfies the boundary condition $\Pi(R,\theta_T \pm \epsilon_T) = 1$, we impose

$$\langle \mathbf{T}_T\rangle(\mathbf{r}_O) = \begin{cases} \mathbf{t}_{\epsilon_T}(R,\theta_T + \epsilon_O), & \theta_T < 0, \\ \mathbf{t}_{\epsilon_T}(R,\theta_T - \epsilon_O), & \theta_T > 0, \end{cases} \tag{15}$$

$$\langle \mathbf{T}_O\rangle(\mathbf{r}_T) = \begin{cases} \mathbf{t}_{\epsilon_O}(R,\theta_T + \epsilon_T), & \theta_T < 0, \\ \mathbf{t}_{\epsilon_O}(R,\theta_T - \epsilon_T), & \theta_T > 0. \end{cases} \tag{16}$$

Here $\mathbf{t}_\epsilon(r,\theta)$ stands for the MFPT to reach a 2ϵ-extended target located in $(R,0)$ starting from (r,θ). One can show that this definition leads to an exact solution for $\lambda = 0$.

One can then write the splitting probability explicitly as

$$\Pi(\mathbf{r}_S) = \frac{\mathbf{t}_{\epsilon_T}(R,\theta_T + \epsilon_O) + \mathbf{t}_{\epsilon_O}(r,\theta) - \mathbf{t}_{\epsilon_T}(r,|\theta - \theta_T|)}{\mathbf{t}_{\epsilon_T}(R,\theta_T + \epsilon_O) + \mathbf{t}_{\epsilon_O}(R,\theta_T + \epsilon_T)} \tag{17}$$

for $\theta_T + \epsilon_T < \theta$, and

$$\Pi(\mathbf{r}_S) = \frac{\mathbf{t}_{\epsilon_T}(R,\theta_T - \epsilon_O) + \mathbf{t}_{\epsilon_O}(r,\theta) - \mathbf{t}_{\epsilon_T}(r,|\theta - \theta_T|)}{\mathbf{t}_{\epsilon_T}(R,\theta_T - \epsilon_O) + \mathbf{t}_{\epsilon_O}(R,\theta_T - \epsilon_T)} \tag{18}$$

for $\theta_T - \epsilon_T > \theta$.

At this stage, one can employ the exact expression of $\mathbf{t}_\epsilon(r,\theta)$ derived in [12], which involves the numerical inversion of an infinite-dimensional matrix (see Appendix B). Alternatively, one can find in [12] an approximate but fully explicit expression of $\mathbf{t}_\epsilon(r,\theta)$, which is exact for pointlike targets and was shown (in the case $r = R$) to be accurate also for extended targets. This approximation is given here for an arbitrary starting position (r,θ) for the sake of completeness:

$$\mathbf{t}_\epsilon(r,\theta) = \frac{R^2 - r^2}{4D_2} + \frac{R^2}{D_1}\left(1 + \lambda R^2\frac{1-x^2}{4D_2}\right)\psi(r,\theta), \tag{19}$$

where

$$\psi(r,\theta) \simeq \epsilon(\epsilon - \pi) + \frac{1}{3\pi}(\pi^3 - \epsilon^3) - \frac{2\omega^2}{\pi^2}\sum_{k=1}^{\infty}\frac{L_k(\epsilon,\omega,x)}{k}[\sin k\epsilon + k(\pi - \epsilon)\cos k\epsilon]$$
$$+ \frac{2}{\pi}\sum_{n=1}^{\infty}\left(\frac{r}{R}\right)^n\left(\frac{\omega^2}{\pi}\left[\sum_{k=1}^{\infty}L_k(\epsilon,\omega,x)I_{kn}\right] - \frac{\sin n\epsilon + n(\pi - \epsilon)\cos n\epsilon}{n^3}\right)\cos n\theta, \tag{20}$$

with $\omega^2 = R^2\lambda/D_1$, $x = 1 - a/R$, and

$$I_{kn} = (1 - \delta_{k,n})\frac{2k}{n^3 - k^2 n}(n\cos n\epsilon\sin k\epsilon - k\cos k\epsilon\sin n\epsilon) + \delta_{k,n}\left(\pi - \epsilon + \frac{\sin 2k\epsilon}{2k}\right),$$

$$L_k(\epsilon,\omega,x) = \frac{(1 - x^k)(k(\pi - \epsilon)\cos k\epsilon + \sin k\epsilon)}{k^3\left[k^2 + \frac{\omega^2}{\pi}(1 - x^k)\left(\pi - \epsilon + \frac{\sin 2k\epsilon}{2k}\right)\right]}.$$

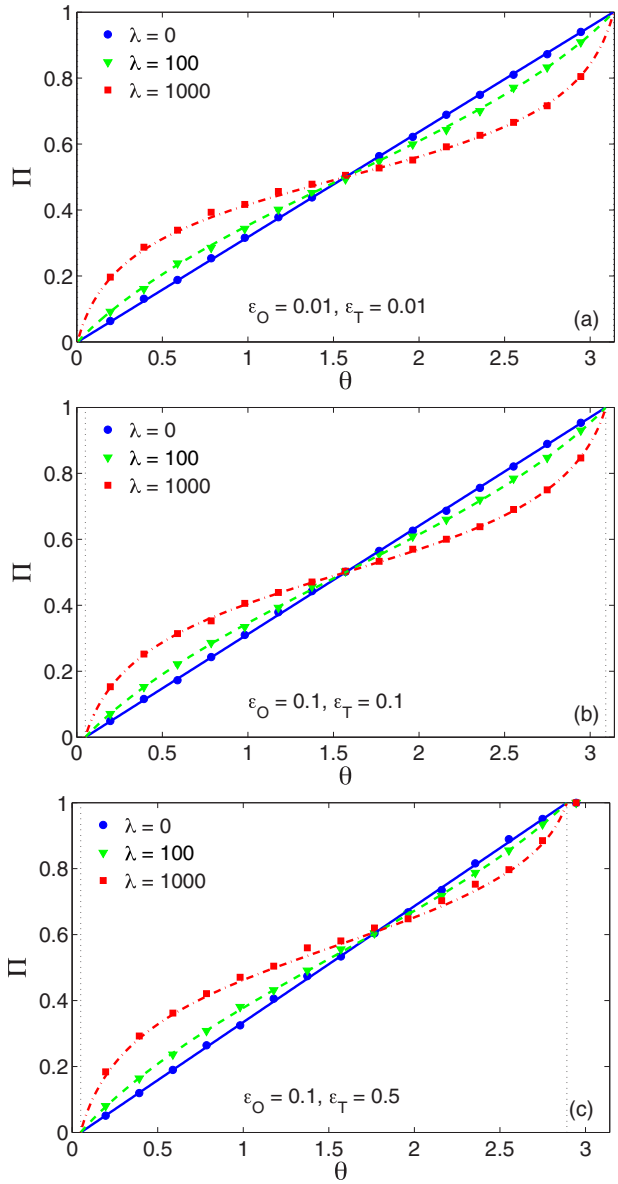

FIG. 2. (Color online) Splitting probability to reach the target T of angular extension ϵ_T placed in (R,π) before the target O of angular extension ϵ_O placed in $(R,0)$, as a function of the starting angle θ, in two dimensions, with $a = 0.01R$, three values of λ, and (a) $\epsilon_O = \epsilon_T = 0.01$, (b) $\epsilon_O = \epsilon_T = 0.1$, and (c) $\epsilon_O = 0.1$, $\epsilon_T = 0.5$. Lines stand for theoretical formula (17) (in which we used the exact expression of the MFPT), while symbols stand for Monte Carlo simulations. Note that approximate expressions (not shown) resulting from Eqs. (19) and (20) almost coincide with the exact ones.

Several comments are in order:

(i) One can show that the limits $\epsilon_T \to 0$ and $\epsilon_O \to 0$ yield the exact result for $\Pi(\mathbf{r}_S)$, explicitly derived in Appendix A.

(ii) Figure 2 shows that the splitting probability obtained by Monte Carlo simulations (see Appendix D) is in excellent agreement with Eq. (14), where the MFPTs are computed according to the exact expression reminded in Appendix B, both for targets of identical [Figs. 2(a) and 2(b)] and different [Fig. 2(c)] extensions. Note that the agreement holds even for large values of ϵ_O and ϵ_T.

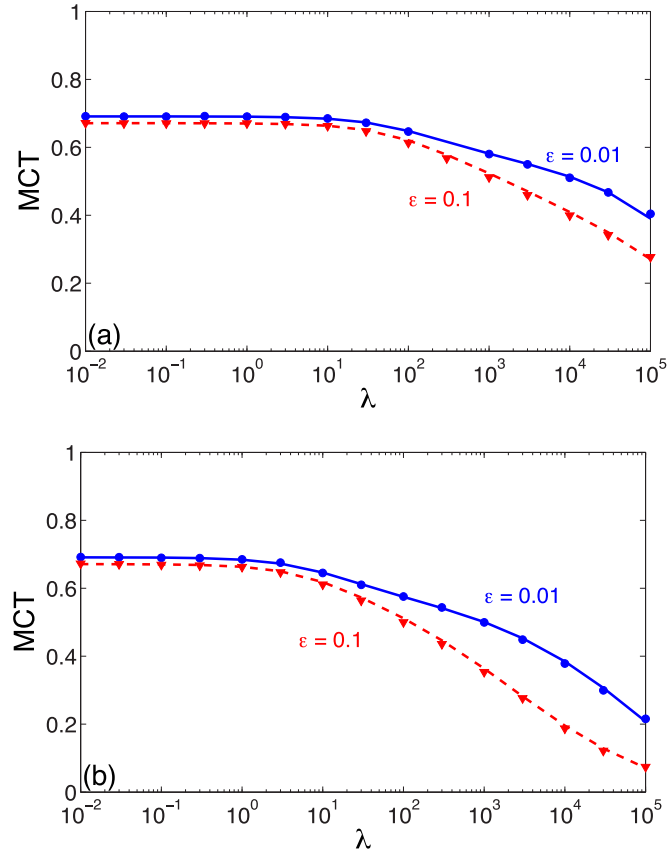

FIG. 3. (Color online) The normalized MCT $\langle \mathcal{C}(\mathbf{r}_S)\rangle$ in two dimensions as a function of the desorption rate λ, with $D_1 = 1$ (arb. units), $R = 1$ (arb. units), and the starting point at (R,π) ("crossing" case), with (a) $a = 0.01R$ and (b) $a = 0.1R$. Two angular sizes of the opening, $\epsilon_O = \epsilon$, are 0.01 (blue solid line) and 0.1 (red dashed line), with $\epsilon_T = 0$. Lines show the results of Eqs. (1) and (17), where exact expressions of the MFPTs have been used, while symbols stand for Monte Carlo simulations.

(iii) The calculation of the splitting probability $\Pi(\mathbf{r}_S)$ gives access to the mean covered territory $\langle \mathcal{C}(\mathbf{r}_S)\rangle$ according to Eq. (1). In the 2D case, we can simply consider $\epsilon_T = 0$ (and $\epsilon_O = \epsilon$). These results show that the MCT exhibits very different dependencies on λ which are controlled by the position of the starting point $\mathbf{r}_S$, as illustrated in Figs. 3 and 4. In the case of crossing when the particle starts from a point (R,π) opposite to the exit, the mean covered territory $\langle \mathcal{C}(\mathbf{r}_S)\rangle$ is a monotonically decreasing function of the desorption rate λ. In the opposite case of return when the particle enters and exits the domain by the same zone [the starting point being set at $(R,\epsilon + a)$, at a distance a from the opening O], $\langle \mathcal{C}(\mathbf{r}_S)\rangle$ is on the contrary an increasing function of λ for small λ: the bulk excursions tend to prevent the particle from being localized in the neighborhood of the opening O and favor longer trajectories. For larger values of λ the probability to reach a pointlike target T before the extended opening O vanishes, and $\langle \mathcal{C}(\mathbf{r}_S)\rangle$ eventually becomes a decreasing function of the desorption rate. The combination of both effects for intermediate values of λ yields a nonmonotonic variation. Finally, $\langle \mathcal{C}(\mathbf{r}_S)\rangle$ can also be a nonmonotonic function of λ for other specific regions of the starting points, as illustrated in

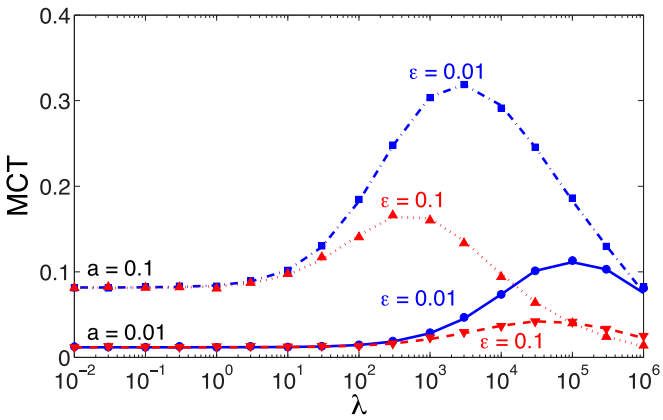

FIG. 4. (Color online) The normalized MCT $\langle \mathcal{C}(\mathbf{r}_S)\rangle$ in two dimensions as a function of the desorption rate λ, with $D_1 = 1$ (arb. units), $R = 1$ (arb. units), the starting point in $(R,a+\epsilon)$ ("return" case), and two choices both for a ($a = 0.1R$ and $a = 0.01R$) and $\epsilon_O = \epsilon$ ($\epsilon = 0.1$ and $\epsilon = 0.01$), with $\epsilon_T = 0$. Lines show theoretical results of Eqs. (1) and (17), while symbols stand for Monte Carlo simulations.

Fig. 5. Note that such nonmonotonic behavior can also occur in the case of a target T with nonzero extension: $\epsilon_T > 0$. Indeed, the first argument for making $\langle \mathcal{C}(\mathbf{r}_S)\rangle$ an increasing function of λ for small λ is still valid, and by taking ϵ_T small enough (but not zero), it is clear that $\Pi(\mathbf{r}_S)$ can be arbitrarily small in the limit $\lambda \to \infty$, so that $\langle \mathcal{C}(\mathbf{r}_S)\rangle$ is a decreasing function of λ for large λ. This nonmonotonic behavior is seen in Fig. 5. Such optimization of the MCT, already pointed out in the case of pointlike targets, can have important applications in the context of heterogeneous catalysis [23].

B. Three-dimensional case

We consider now the target O defined by the sector of the sphere $\theta \in [0,\epsilon_O]$, where θ is the elevation angle in standard

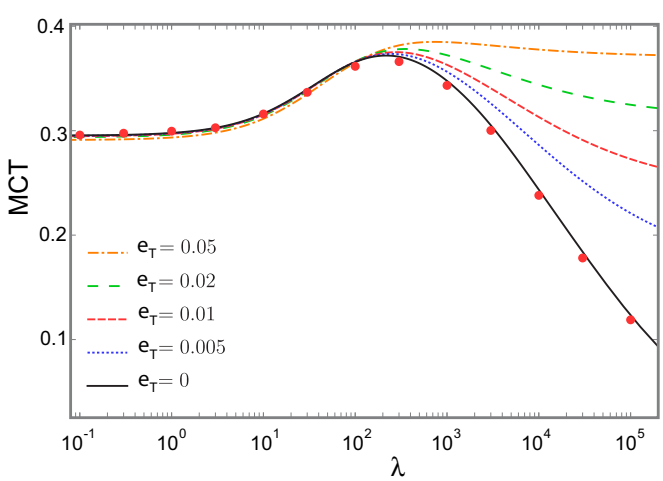

FIG. 5. (Color online) The normalized MCT $\langle \mathcal{C}(\mathbf{r}_S)\rangle$ in two dimensions as a function of the desorption rate λ, with $D_1 = 1$ (arb. units), $R = 1$ (arb. units), $\epsilon_O = 0.05$, and $a = 0.05R$, for a particle starting from a "middle" position: $(R,0.6)$. Lines show theoretical results of Eqs. (1), (17), and (18), while symbols stand for Monte Carlo simulations in the case $\epsilon_T = 0$.

spherical coordinates. We define the second angle ϕ of the standard spherical coordinates so that $S \equiv (r,\theta,\phi = 0)$.

In the 3D case, the definition of the covered territory requires the introduction of a finite angular particle size ϵ; this is equivalent to consider a target $T \equiv (R,\theta_T,\phi_T)$ of angular extension $\epsilon_T = \epsilon$.

For the sake of simplicity, we consider here two kinds of trajectories: the crossing trajectories [starting from the south pole $(R,\theta_S = \pi)$] and the return trajectories [starting from the north pole $(R-a,\theta_S = 0)$]. In both cases, there is no dependence on ϕ so that

$$\langle \mathcal{C}(\mathbf{r}_S)\rangle = 2\pi R^2 \int_\epsilon^\pi \Pi(\mathbf{r}_S)\sin\theta_T d\theta_T. \tag{21}$$

As in the 2D case, we now use Eq. (14) to express the splitting probability in terms of the MFPT. Denoting $\mathbf{t}_\epsilon(r,\theta)$ the MFPT to reach a target of extension ϵ located at $(R,0)$ starting from (r,θ,ψ), the splitting probability can be written as

$$\Pi(\mathbf{r}_S) = \frac{\mathbf{t}_{\epsilon_T}(R,\theta_T) + \mathbf{t}_{\epsilon_O}(r,\theta_S) - \mathbf{t}_{\epsilon_T}(r,|\theta_S - \theta_T|)}{\mathbf{t}_{\epsilon_T}(R,\theta_T) + \mathbf{t}_{\epsilon_O}(R,\theta_T)}. \tag{22}$$

Exact expressions of the MFPTs to the extended targets (either T or O) involved in Eq. (22) have been derived in [12] and are summarized in Appendix C. As in the 2D case, one can employ either exact expressions (which involve numerical matrix inversions), or explicit approximate formulas for the MFPT from a starting point (R,θ) to reach a target of extension ϵ at $(R,0)$, which we recall here:

$$\mathbf{t}_\epsilon(R,\theta) = \frac{R^2}{D_1}\left(1 + \lambda R^2 \frac{1-x^2}{6D_2}\right)\psi(\theta), \tag{23}$$

where

$$\psi(\theta) \approx \ln\left(\frac{1-\cos\theta}{1-\cos\epsilon}\right) + \frac{\omega^2}{2}\sum_{n=1}^{\infty}(1-x^n)\frac{2n+1}{n(n+1)}[P_n(\cos\theta) - P_n(\cos\epsilon)] \times \frac{\left(1+\frac{n\cos\epsilon}{n+1}\right)P_n(\cos\epsilon) + \frac{P_{n-1}(\cos\epsilon)}{n+1}}{n(n+1) + \frac{\omega^2}{2}(1-x^n)(2n+1)I_\epsilon(n,n)}, \tag{24}$$

with

$$I_\epsilon(n,n) = \int_{-1}^{\cos\epsilon} P_n(u)\,[P_n(u) - P_n(\cos\epsilon)]\,du,$$

and where $P_n(z)$ are Legendre polynomials. Note that we here took $r = R$ for the sake of readability. These expressions allow us to compute explicitly the splitting probability $\Pi(\mathbf{r}_S)$, and hence the MCT.

Several comments are in order:

(i) We performed Monte Carlo simulations in order to check the accuracy of the analytical approximations. To speed up simulations of surface-mediated diffusion, the bulk phases have been taken into account by using the harmonic measure density which is explicitly known in the case of spheres. A more detailed description of the algorithm is given in Appendix D.

(ii) Figure 6 illustrates an excellent agreement between the splitting probabilities obtained numerically by Monte

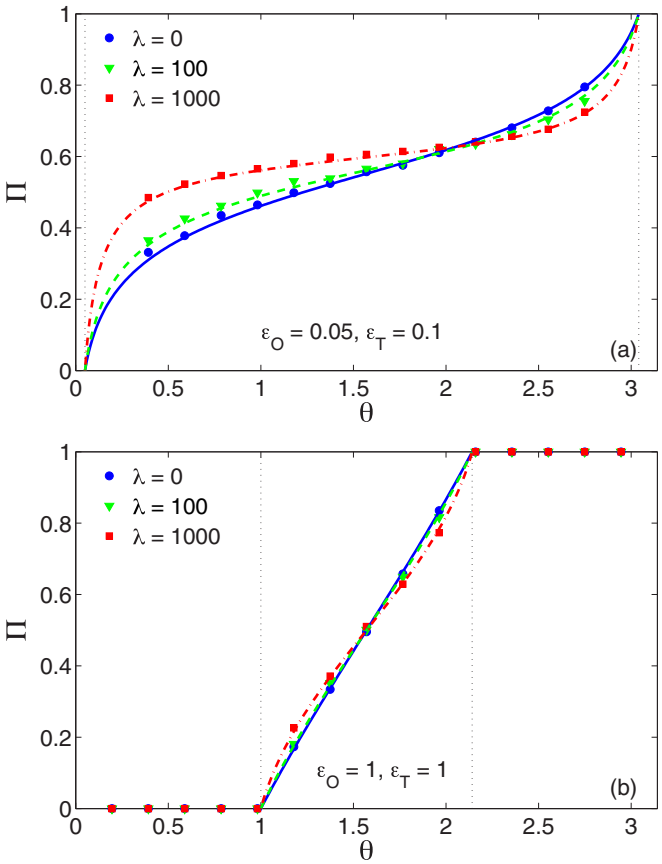

FIG. 6. (Color online) The splitting probability to reach the target T of angular extension ϵ_T placed in (R,π) before the target O of angular extension ϵ_O placed in $(R,0)$, as a function of the starting angle θ, in three dimensions, with $D_1 = 1$ (arb. units), $R = 1$ (arb. units), and $a = 0.01R$, three values of λ, and (a) $\epsilon_O = 0.05$, $\epsilon_T = 0.1$, and (b) $\epsilon_O = \epsilon_T = 1$. Lines stand for theoretical formula (22) (in which the exact expressions for MPFTs were used), while symbols stand for Monte Carlo simulations.

Carlo simulations with the prediction of Eq. (14), where the MFPTs are computed using the exact expression reminded in Appendix C, both in the case of targets of identical [Fig. 6(b)] and different [Fig. 6(a)] extensions. Note that the agreement holds even for large values of ϵ_O,ϵ_T [Fig. 6(b)].

(iii) These calculations of the splitting probability $\Pi(\mathbf{r}_S)$ give access to the mean covered territory $\langle \mathcal{C}(\mathbf{r}_S)\rangle$ according to Eq. (1). For the sake of simplicity, we just consider here the case $\epsilon_T = \epsilon_O = \epsilon$. Note that it can also be understood as the case of an extended particle (of radius ϵ) and two pointlike targets O and T. As in the 2D case, the MCT exhibits different dependencies on λ controlled by the position of the starting point $\mathbf{r}_S$, as illustrated on Fig. 7: the MCT is decreasing with λ in the case of crossing and increasing with λ in the case of return. Note that, in contrast to the 2D case, here both targets T and O are considered to have the same spatial extension, so that the splitting probability to reach T does not vanish when $\lambda \to \infty$. However, as in the 2D case, by taking ϵ_T small enough, the splitting probability to reach T can be arbitrarily small when $\lambda \to \infty$, so that the optimization of the MCT is also possible in three dimensions.

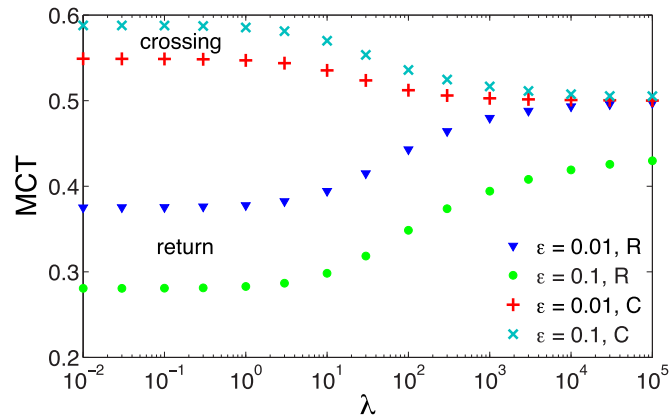

FIG. 7. (Color online) The normalized MCT $\langle \mathcal{C}(\mathbf{r}_S)\rangle$ in three dimensions as a function of the desorption rate λ, with $D_1 = 1$ (arb. units), $R = 1$ (arb. units), $a = 0.1R$, and $\epsilon_O = \epsilon_T = \epsilon$. Two upper curves correspond to the crossing case [i.e., starting from (R,π)], while two lower curves correspond to the return case [i.e., starting from $(R-a,0)$]. In both cases, the MCT for $\epsilon = 0.01$ is larger than for $\epsilon = 0.1$, as expected. Exact expressions for the MFPT have been used.

V. CONCLUSION

In conclusion, we have considered the mean territory covered by a particle that performs surface-mediated diffusion inside a spherical confining domain (in two and three dimensions) before its exit through an opening on the surface. We have derived a general formula that relates the splitting probability between two targets on the surface, to the mean first passage time to a single target that has been recently calculated for such surface-mediated diffusion processes. This formula is exact for pointlike targets and holds for domains of arbitrary shapes in two dimensions; we have checked numerically that it is also accurate for extended targets in 2D and 3D spherical domains. The determination of the mean covered territory, made possible by the calculation of splitting probabilities, showed that it can be a nonmonotonic function of the desorption rate.

ACKNOWLEDGMENTS

Support from the European Research Council starting Grant No. FPTOpt-277998 and the French National Research Agency (ANR) Grants Micemico and DynRec are acknowledged.

APPENDIX A: EXACT CALCULATION OF THE 2D SPLITTING PROBABILITY FOR $\epsilon = 0$

In this Appendix, we present a detailed derivation of an exact representation for the splitting probability $\Pi(r,\theta)$ to reach the target at (R,θ_T) before exiting the disk through the target at $(R,0)$, when started from (r,θ). Both targets are pointlike (i.e., $\epsilon_O = \epsilon_T = \epsilon = 0$).

We introduce two splitting probabilities, $\Pi_1(\theta)$ and $\Pi_2(r,\theta)$, for the starting point belonging to the boundary [i.e., (R,θ)] and to the interior of the disk [i.e., (r,θ)], respectively.

These splitting probabilities satisfy coupled partial differential equations (PDEs)

$$\Pi_1''(\theta) - \omega^2(\Pi_1(\theta) - \Pi_2(R-a,\theta)) = 0, \tag{A1}$$

$$\Delta_2 \Pi_2(r,\theta) = 0, \tag{A2}$$

where $\omega^2 = R^2\lambda/D_1$. In Eq. (A1), the second term describes random desorption events (ejection of a particle at distance a from the boundary). These equations are completed by the following boundary conditions:

$$\Pi_2(R,\theta) = \Pi_1(\theta), \tag{A3}$$

$$\Pi_1(0) = \Pi_1(2\pi) = 0, \tag{A4}$$

$$\Pi_1(\theta_T) = 1. \tag{A5}$$

To solve Eqs. (A1) and (A2), we introduce the Green function $G(\theta,\theta')$ on the circle,

$$G''(\theta,\theta') - \omega^2 G(\theta,\theta') = \delta(\theta-\theta'), \tag{A6}$$

with Dirichlet boundary condition $G(0,\theta') = G(2\pi,\theta') = 0$.

Rewriting Eq. (A1) as

$$\Pi_1''(\theta) - \omega^2\Pi_1(\theta) = -\omega^2\Pi_2(R-a,\theta),$$

one gets

$$\Pi_1(\theta) = h(\theta) + \int_0^{2\pi} G(\theta,\theta')[-\omega^2\Pi_2(R-a,\theta')]d\theta', \tag{A7}$$

where $h(\theta)$ is the solution of the homogeneous equation $h''(\theta) - \omega^2 h(\theta) = 0$ with the boundary conditions $h(0) = h(2\pi) = 0$ and $h(\theta_T) = 1$ [31]:

$$h(\theta) = \frac{\sinh(\omega\min\{\theta,\theta_T\})\sinh(\omega(2\pi - \max\{\theta,\theta_T\}))}{\sinh(\omega\theta_T)\sinh(\omega(2\pi-\theta_T))}. \tag{A8}$$

A general solution of Eq. (A2) can be written as

$$\Pi_2(r,\theta) = \alpha_0 + \sum_{n=1}^{\infty} r^n\left[\alpha_n\cos(n\theta) + \beta_n\sin(n\theta)\right], \tag{A9}$$

with the unknown coefficients α_n and β_n to be determined.

1. Solution for $\theta \in [0,\theta_T]$

When $\theta \in [0,\theta_T]$, the Green function is

$$G(\theta,\theta') = -\frac{\sinh(\omega\min\{\theta,\theta'\})\sinh(\omega(\theta_T - \max\{\theta,\theta'\}))}{\omega\sinh(\omega\theta_T)} \tag{A10}$$

for any $\theta' \in [0,\theta_T]$, and zero otherwise. The splitting probability reads

$$\Pi_1(\theta) = \frac{\sinh(\omega\theta)}{\sinh(\omega\theta_T)} + \frac{\omega}{\sinh(\omega\theta_T)}\int_0^{\theta_T}\sinh(\omega\min\{\theta,\theta'\}) \times \sinh(\omega(\theta_T - \max\{\theta,\theta'\}))\Pi_2(R-a,\theta')d\theta'. \tag{A11}$$

Splitting the integration interval $[0,\theta_T]$ into two subintervals, $[0,\theta]$ and $[\theta,\theta_T]$, and substituting Eq. (A9), one gets

$$\Pi_1(\theta) = \frac{\sinh(\omega\theta)}{\sinh(\omega\theta_T)} + \frac{\omega A(\theta)}{\sinh(\omega\theta_T)}, \tag{A12}$$

with

$$A(\theta) = \alpha_0 N_0(0,\theta,\theta_T) + \sum_{n=1}^{\infty}(R-a)^n(\alpha_n N_n(0,\theta,\theta_T) + \beta_n O_n(0,\theta,\theta_T)), \tag{A13}$$

where we introduced the following notations:

$$J_n(\theta_-,\theta) \equiv \int_{\theta_-}^{\theta}\sinh(\omega(\theta'-\theta_-))\cos(n\theta')d\theta',$$

$$K_n(\theta,\theta_+) \equiv \int_{\theta}^{\theta_+}\sinh(\omega(\theta_+-\theta'))\cos(n\theta')d\theta',$$

$$L_n(\theta_-,\theta) \equiv \int_{\theta_-}^{\theta}\sinh(\omega(\theta'-\theta_-))\sin(n\theta')d\theta',$$

$$M_n(\theta,\theta_+) \equiv \int_{\theta}^{\theta_+}\sinh(\omega(\theta_+-\theta'))\sin(n\theta')d\theta',$$

$$N_n(\theta_-,\theta,\theta_+) \equiv \sinh(\omega(\theta_+-\theta))J_n(\theta_-,\theta) + \sinh(\omega(\theta-\theta_-))K_n(\theta,\theta_+),$$

$$O_n(\theta_-,\theta,\theta_+) \equiv \sinh(\omega(\theta_+-\theta))L_n(\theta_-,\theta) + \sinh(\omega(\theta-\theta_-))M_n(\theta,\theta_+).$$

After simplification, one gets

$$\begin{aligned}\omega A(\theta) = {} & \alpha_0[\sinh(\omega\theta_T) - \sinh(\omega\theta) - \sinh(\omega(\theta_T-\theta))] \\ & + \sum_{n=1}^{\infty} k_n[\alpha_n(\sinh(\omega\theta_T)\cos(n\theta) - \cos(n\theta_T)\sinh(\omega\theta) \\ & + \sinh(\omega(\theta-\theta_T))) \\ & + \beta_n(\sinh(\omega\theta_T)\sin(n\theta) - \sin(n\theta_T)\sinh(\omega\theta))],\end{aligned}$$

where

$$k_n \equiv (R-a)^n\frac{\omega^2}{\omega^2+n^2}. \tag{A14}$$

Denoting

$$F(\theta) \equiv \sum_{n=1}^{\infty} k_n[\alpha_n\cos(n\theta) + \beta_n\sin(n\theta)], \tag{A15}$$

$$S \equiv \alpha_0 + \sum_{n=1}^{\infty} k_n\alpha_n, \tag{A16}$$

Eq. (A12) becomes

$$\Pi_1(\theta) = \alpha_0 + F(\theta) + \lambda(\theta_T)\sinh(\omega\theta) + \mu(\theta_T)\sinh(\omega(\theta_T-\theta)), \tag{A17}$$

with

$$\lambda(\theta_T) \equiv -\frac{\alpha_0 - 1 + F(\theta_T)}{\sinh(\omega\theta_T)}, \tag{A18}$$

$$\mu(\theta_T) \equiv -\frac{S}{\sinh(\omega\theta_T)}. \tag{A19}$$

2. Solution for $\theta \in [\theta_T, 2\pi]$

Similarly, one can solve the problem when $\theta \in [\theta_T, 2\pi]$. The Green function reads

$$G(\theta,\theta') = -\frac{\sinh(\omega(\min\{\theta,\theta'\} - \theta_T)\sinh(\omega(2\pi - \max\{\theta,\theta'\}))}{\omega\sinh(\omega(2\pi - \theta_T))} \tag{A20}$$

for $\theta' \in [\theta_T, 2\pi]$, and zero otherwise. One finds

$$\Pi_1(\theta) = \frac{\sinh(\omega(2\pi - \theta))}{\sinh(\omega(2\pi - \theta_T))} + \frac{\omega}{\sinh(\omega(2\pi - \theta_T))}\int_{\theta_T}^{2\pi} \sinh(\omega(\min\{\theta,\theta'\} - \theta_T))\sinh(\omega(2\pi - \max\{\theta,\theta'\}))\Pi_2(R-a,\theta')d\theta', \tag{A21}$$

from which

$$\Pi_1(\theta) = \frac{\sinh(\omega(2\pi - \theta))}{\sinh(\omega(2\pi - \theta_T))} + \frac{\omega B(\theta)}{\sinh(\omega(2\pi - \theta_T))}, \tag{A22}$$

with

$$B(\theta) = \alpha_0 N_0(\theta_T,\theta,2\pi) + \sum_{n=1}^{\infty}(R-a)^n[\alpha_n N_n(\theta_T,2\pi) + \beta_n O_n(\theta_T,\theta,2\pi)] \tag{A23}$$

that can be simplified to

$$\begin{aligned}\omega B(\theta) = {} & \alpha_0[\sinh(\omega(2\pi - \theta_T)) - \sinh(\omega(\theta - \theta_T)) - \sinh(\omega(2\pi - \theta))] \\ & + \sum_{n=1}^{\infty} k_n[\alpha_n(\sinh(\omega(2\pi - \theta_T))\cos(n\theta) - \cos(n\theta_T)\sinh(\omega(2\pi - \theta)) - \sinh(\omega(\theta - \theta_T))) \\ & + \beta_n(\sinh(\omega(2\pi - \theta_T))\sin(n\theta) - \sin(n\theta_T)\sinh(\omega(2\pi - \theta)))].\end{aligned}$$

One gets, therefore,

$$\Pi_1(\theta) = \alpha_0 + F(\theta) + \eta(\theta_T)\sinh(\omega(2\pi - \theta)) + \nu(\theta_T)\sinh(\omega(\theta - \theta_T)), \tag{A24}$$

with

$$\eta(\theta_T) \equiv -\frac{\alpha_0 - 1 + F(\theta_T)}{\sinh(\omega(2\pi - \theta_T))}, \quad \nu(\theta_T) \equiv -\frac{S}{\sinh(\omega(2\pi - \theta_T))}.$$

Combining Eqs. (A17) and (A24), one can write the splitting probability as

$$\Pi_1(\theta) = \alpha_0 + F(\theta) + H(\theta), \tag{A25}$$

where

$$H(\theta) = \begin{cases} \lambda(\theta_T)\sinh(\omega\theta) + \mu(\theta_T)\sinh(\omega(\theta_T - \theta)), & (0 < \theta < \theta_T), \\ \eta(\theta_T)\sinh(\omega(2\pi - \theta)) + \nu(\theta_T)\sinh(\omega(\theta - \theta_T)), & (\theta_T < \theta < 2\pi). \end{cases} \tag{A26}$$

A Fourier series expansion of $H(\theta)$ is

$$H(\theta) = a_0 + \sum_{n=1}^{\infty}[a_n\cos(n\theta) + b_n\sin(n\theta)], \tag{A27}$$

with the explicit coefficients a_n and b_n:

$$\begin{aligned} a_0 &= \frac{1}{2\pi}[\lambda(\theta_T)J_0(0,\theta_T) + \mu(\theta_T)K_0(0,\theta_T) + \nu(\theta_T)J_0(\theta_T,2\pi) + \eta(\theta_T)K_0(\theta_T,2\pi)], \\ a_n &= \frac{1}{\pi}[\lambda(\theta_T)J_n(0,\theta_T) + \mu(\theta_T)K_n(0,\theta_T) + \nu(\theta_T)J_n(\theta_T,2\pi) + \eta(\theta_T)K_n(\theta_T,2\pi)], \\ b_n &= \frac{1}{\pi}[\lambda(\theta_T)L_n(0,\theta_T) + \mu(\theta_T)M_n(0,\theta_T) + \nu(\theta_T)L_n(\theta_T,2\pi) + \eta(\theta_T)M_n(\theta_T,2\pi)]. \end{aligned}$$

Simplifications yield

$$\begin{aligned} 2\pi\omega a_0 &= [\lambda(\theta_T) + \mu(\theta_T)][\cosh(\omega\theta_T) - 1] + [\nu(\theta_T) + \eta(\theta_T)][\cosh(\omega(2\pi - \theta_T)) - 1] \\ &= C\left(\frac{1 - \cosh(\omega\theta_T)}{\sinh(\omega\theta_T)} + \frac{1 - \cosh(\omega(2\pi - \theta_T))}{\sinh(\omega(2\pi - \theta_T))}\right), \end{aligned} \tag{A28}$$

where

$$C \equiv \alpha_0 - 1 + F(\theta_T) + S. \tag{A29}$$

The other coefficients are

$$\begin{aligned}(\omega^2+n^2)\pi a_n &= \lambda(\theta_T)[-\omega + \omega\cosh(\omega\theta_T)\cos(n\theta_T) + n\sinh(\omega\theta_T)\sin(n\theta_T)]\\ &\quad + \mu(\theta_T)\omega[\cosh(\omega\theta_T) - \cos(n\theta_T)] + \nu(\theta_T)\omega[\cosh(\omega(2\pi-\theta_T)) - \cos(n\theta_T)]\\ &\quad + \eta(\theta_T)[-\omega + \omega\cosh(\omega(2\pi-\theta_T))\cos(n\theta_T) - n\sinh(\omega(2\pi-\theta_T))\sin(n\theta_T)]\\ &= \frac{\omega}{\sinh(\omega\theta_T)\sinh(\omega(2\pi-\theta_T))}[(C-S)(\sinh(\omega\theta_T) + \sinh(\omega(2\pi-\theta_T)) - \sinh(2\pi\omega)\cos(n\theta_T))\\ &\quad + S(-\sinh(2\pi\omega) + \cos(n\theta_T)[\sinh(\omega(2\pi-\theta_T)) + \sinh(\omega\theta_T)])],\end{aligned}$$

$$\begin{aligned}(\omega^2+n^2)\pi b_n &= \lambda(\theta_T)[\omega\cosh(\omega\theta_T)\sin(n\theta_T) - n\sinh(\omega\theta_T)\cos(n\theta_T)]\\ &\quad + \mu(\theta_T)[n\sinh(\omega\theta_T) - \omega\sin(n\theta_T)] - \nu(\theta_T)[n\sinh(\omega(2\pi-\theta_T)) + \omega\sin(n\theta_T)]\\ &\quad + \eta(\theta_T)[\omega\cosh(\omega(2\pi-\theta_T))\sin(n\theta_T) + n\sinh(\omega(2\pi-\theta_T))\cos(n\theta_T)]\\ &= \frac{\omega}{\sinh(\omega\theta_T)\sinh(\omega(2\pi-\theta_T))}[(C-S)(-\sinh(2\pi\omega)\sin(n\theta_T)) + S\sin(n\theta_T)[\sinh(\omega(2\pi-\theta_T)) + \sinh(\omega\theta_T)]].\end{aligned}$$

The coefficients α_n, β_n can be related to a_n, b_n by substituting Eqs. (A9), (A15), and (A27) into the boundary condition (A3):

$$\alpha_0 + \sum_{n=1}^{\infty} R^n[\alpha_n\cos(n\theta) + \beta_n\sin(n\theta)] = \alpha_0 + a_0 + \sum_{n=1}^{\infty}[(a_n + k_n\alpha_n)\cos(n\theta) + (b_n + k_n\beta_n)\sin(n\theta)]. \tag{A30}$$

This identity implies the following relations:

$$a_0 = 0, \quad a_n = (R^n - k_n)\alpha_n, \quad b_n = (R^n - k_n)\beta_n. \tag{A31}$$

From the first relation, one gets $C = 0$ according to Eq. (A28), from which

$$\alpha_0 = 1 - F(\theta_T) - S. \tag{A32}$$

That yields a simplification for the other coefficients

$$a_n = \frac{\omega S(\cos(n\theta_T) - 1)(\sinh(\omega\theta_T) + \sinh(\omega(2\pi-\theta_T)) + \sinh(2\pi\omega))}{\pi(\omega^2+n^2)\sinh(\omega\theta_T)\sinh(\omega(2\pi-\theta_T))} = \frac{\cos(n\theta_T) - 1}{\sin(n\theta_T)}b_n, \tag{A33}$$

from which

$$\alpha_n = \frac{\cos(n\theta_T) - 1}{\sin(n\theta_T)}\beta_n. \tag{A34}$$

Substituting Eqs. (A15), (A16), and (A34) into Eq. (A32), one gets

$$\alpha_0 = 1 - \alpha_0 - \sum_{n=1}^{\infty} k_n\alpha_n\left[\cos(n\theta_T) + 1 + \frac{\sin^2(n\theta_T)}{\cos(n\theta_T) - 1}\right],$$

in which all the terms in the sum are zero. One concludes that

$$\alpha_0 = \frac{1}{2}. \tag{A35}$$

Writing

$$g(\theta_T) = \omega\frac{\sinh(\omega\theta_T) + \sinh(\omega(2\pi-\theta_T)) + \sinh(2\pi\omega)}{\pi\sinh(\omega\theta_T)\sinh(\omega(2\pi-\theta_T))},$$

one gets

$$\alpha_n = Sg(\theta_T)\frac{\cos(n\theta_T) - 1}{(R^n - k_n)(\omega^2+n^2)}.$$

Using the definition of S in Eq. (A16), one finds

$$S(\theta_T) = \frac{\alpha_0}{1 - g(\theta_T)\sum_{n=1}^{\infty}\frac{k_n}{R^n - k_n}\frac{\cos(n\theta_T)-1}{\omega^2+n^2}}.$$

We obtain, therefore,

$$\alpha_n = \frac{T(\theta_T)}{2}\frac{\cos(n\theta_T) - 1}{(R^n - k_n)(\omega^2+n^2)},$$

$$\beta_n = \frac{T(\theta_T)}{2}\frac{\sin(n\theta_T)}{(R^n - k_n)(\omega^2+n^2)},$$

where

$$T(\theta_T) \equiv 2S(\theta_T)g(\theta_T) = \frac{g(\theta_T)}{1 - g(\theta_T)\sum_{n=1}^{\infty}\frac{k_n}{R^n - k_n}\frac{\cos(n\theta_T)-1}{\omega^2+n^2}}.$$

Finally one gets

$$\Pi(r,\theta) = \frac{1}{2} + T(\theta_T)\sum_{n=1}^{\infty}\frac{(r/R)^n}{(1-k_n)(\omega^2+n^2)}\sin(n\theta_T/2) \times \sin(n(\theta - \theta_T/2)), \tag{A36}$$

where

$$T(\theta_T) \equiv \frac{g(\theta_T)}{1 - g(\theta_T)\sum_{n\geqslant 1}\frac{k_n}{1-k_n}\frac{\cos n\theta_T - 1}{\omega^2+n^2}},$$
$$g(\theta_T) \equiv \omega\frac{\sinh\omega\theta_T + \sinh\omega(2\pi-\theta_T) + \sinh 2\pi\omega}{\pi\sinh\omega\theta_T\sinh\omega(2\pi-\theta_T)},$$
$$k_n \equiv x^n\frac{\omega^2}{\omega^2+n^2}.$$

APPENDIX B: EXACT RESULT OF THE 2D MFPT FOR $\epsilon \neq 0$

Following [12], the 2D MFPT reads

$$\mathbf{t}_\epsilon(r,\theta) = \frac{R^2-r^2}{4D_2} + \frac{R^2}{D_1}\left(1+\lambda R^2\frac{1-x^2}{4D_2}\right)\psi(r,\theta), \quad \text{(B1)}$$

with

$$\psi(r,\theta) = \alpha_0 + \sum_{n\geqslant 1}\left(\frac{r}{R}\right)^n\alpha_n\cos n\theta \quad \text{(B2)}$$

and

$$\alpha_0 = \frac{1}{2\pi}\int_\epsilon^{2\pi-\epsilon}\psi(R,\theta)\,d\theta,$$
$$\alpha_n = \frac{1}{\pi}\int_\epsilon^{2\pi-\epsilon}\psi(R,\theta)\cos n\theta\,d\theta, \quad \text{(B3)}$$

where

$$\psi(R,\theta) = (\theta-\epsilon)(2\pi-\epsilon-\theta) + \sum_{k\geqslant 1}d_k(\cos k\theta - \cos k\epsilon). \quad \text{(B4)}$$

We introduced the following notations:

$$d_k = \Omega[(I-\Omega Q)^{-1}U]_k \quad (k=1,2,\ldots), \quad \text{(B5)}$$

$$U_k = \frac{x^k-1}{k^2}\int_\epsilon^{2\pi-\epsilon}\cos(k\theta)(\theta-\epsilon)(2\pi-\epsilon-\theta)\,d\theta, \quad \text{(B6)}$$

$$Q_{k,k'} \equiv -\frac{1-x^n}{n^2}I_\epsilon(k,k'), \quad \text{(B7)}$$

$$I_{kk'} = (1-\delta_{k,k'})\frac{2k}{k'^3-k^2k'}(k'\cos k'\epsilon\sin k\epsilon - k\cos k\epsilon\sin k'\epsilon) + \delta_{k,k'}\left(\pi-\epsilon+\frac{\sin 2k\epsilon}{2k}\right), \quad \text{(B8)}$$

$$\Omega \equiv \frac{\omega^2}{\pi}. \quad \text{(B9)}$$

We obtain, therefore,

$$\pi\alpha_0 = \frac{2}{3}(\pi-\epsilon)^3 - \sum_{k\geqslant 1}d_k\left[(\pi-\epsilon)\cos k\epsilon + \frac{\sin k\epsilon}{k}\right],$$
$$\pi\alpha_n = -\frac{4}{n^2}\left[(\pi-\epsilon)\cos n\epsilon + \frac{\sin n\epsilon}{n}\right] + \sum_{k\geqslant 1}d_kI_\epsilon(n,k). \quad \text{(B10)}$$

This eventually provides an exact expression of $\mathbf{t}_\epsilon(r,\theta)$.

The limit $\epsilon \to 0$ yields the following result:

$$\alpha_0 = 4\sum_{k\geqslant 1}\frac{1}{k^2+(1-x^k)\omega^2},$$
$$\alpha_n = -\frac{4}{n^2+(1-x^n)\omega^2}, \quad \text{(B11)}$$

which is consistent with the first order of the perturbative expansion in [12].

APPENDIX C: EXACT RESULT OF THE 3D MFPT FOR $\epsilon \neq 0$

The 3D analogs of Eqs. (B1)–(B3) are

$$\mathbf{t}_\epsilon(r,\theta) = \frac{R^2-r^2}{6D_2} + \frac{R^2}{D_1}\left(1+\lambda R^2\frac{1-x^2}{6D_2}\right)\psi(r,\theta), \quad \text{(C1)}$$

$$\psi(r,\theta) = \alpha_0 + \sum_{n\geqslant 1}\left(\frac{r}{R}\right)^n\alpha_nP_n(\cos n\theta), \quad \text{(C2)}$$

$$\alpha_0 = \frac{1}{2\pi}\int_\epsilon^\pi\sin\theta\,\psi(R,\theta)\,d\theta,$$
$$\alpha_n = \frac{2n+1}{2\pi}\int_\epsilon^\pi\sin\theta\,P_n(\cos\theta)\psi(R,\theta)\,d\theta, \quad \text{(C3)}$$

with the notation

$$\Omega \equiv \frac{\omega^2}{\pi}, \quad \text{(C4)}$$

and $P_n(z)$ stands for the Legendre polynomial of order n. The exact result (given for $r = R$ for simplicity) is then

$$\psi(R,\theta) = \ln\left(\frac{1-\cos\theta}{1-\cos\epsilon}\right) + \sum_{n=1}^\infty d_n[P_n(\cos\theta) - P_n(\cos\epsilon)], \quad \text{(C5)}$$

with

$$d_n = \Omega[(I-\Omega Q)^{-1}U]_n(n=1,2,\ldots), \quad \text{(C6)}$$

and

$$U_n = \frac{(x^n-1)(2n+1)}{n(n+1)}\int_\epsilon^\pi d\theta'\sin(\theta')P_n(\cos\theta') \times \ln\left(\frac{1-\cos\theta'}{1-\cos\epsilon}\right), \quad \text{(C7)}$$

$$Q_{n,n'} \equiv -\frac{(1-x^n)(2n+1)}{n(n+1)}\int_{-1}^{\cos\epsilon}P_n(u) \times [P_{n'}(u) - P_{n'}(\cos\epsilon)]\,du. \quad \text{(C8)}$$

This eventually provides an exact expression of $\mathbf{t}_\epsilon(R,\theta)$. In the same way as in the 2D case, one can use an approximate expression given by

$$\psi(R,\theta) \approx \ln\left(\frac{1-\cos\theta}{1-\cos\epsilon}\right) + \Omega\sum_{n=1}^\infty(1-x^n)\frac{2n+1}{n(n+1)}[P_n(\cos\theta) - P_n(\cos\epsilon)] \times \frac{\left(1+\frac{n\cos\epsilon}{n+1}\right)P_n(\cos\epsilon) + \frac{P_{n-1}(\cos\epsilon)}{n+1}}{n(n+1)+\Omega(1-x^n)(2n+1)I_\epsilon(n,n)}. \quad \text{(C9)}$$

APPENDIX D: NUMERICAL SIMULATIONS

1. Monte Carlo simulation for intermittent processes

To speed up Monte Carlo simulations of surface-mediated diffusion, the relocation during the bulk phase can be incorporated by using the harmonic measure density which is explicitly known for a disk and a sphere.

a. Two-dimensional case

The harmonic measure density $\omega(r,\theta,\theta')$, i.e., the probability density for first hitting the circle at θ' having started at (r,θ), is

$$\omega(r,\theta,\theta') = \frac{1-r^2}{2\pi[1-2r\cos(\theta-\theta')+r^2]} = \frac{1}{2\pi}\left(1+2\sum_{k=1}^{\infty} r^k \cos k(\theta-\theta')\right). \quad \text{(D1)}$$

Suppose that we start at $\theta = 0$. In this case, the new θ' coordinate on the circle can be generated with the probability density $p(\theta') = \omega(r,0,\theta')$, where r is the radius of the starting point in the bulk (typically, $r = 1-a$, a being the reflection distance, and $R = 1$ the radius of the disk). The random angular displacement has the cumulative distribution function

$$F(\theta) = \int_{-\pi}^{\theta} d\theta' p(\theta'), \quad \text{(D2)}$$

for which one finds for $\theta \in (-\pi,\pi)$

$$F(\theta) = \frac{1}{2} + \frac{1}{\pi}\arctan\left(\frac{1+r}{1-r}\tan(\theta/2)\right), \quad \text{(D3)}$$

which increases from 0 at $\theta = -\pi$ to 1 at $\theta = \pi$. The inverse function is given as

$$\theta = 2\arctan\left(\frac{1-r}{1+r}\tan\left(\pi(x-1/2)\right)\right), \quad \text{(D4)}$$

where x ranges between 0 and 1. From a uniform number x, one can easily generate the relocation angle θ.

b. Three-dimensional case

Similarly, the harmonic measure density (given by the Poisson kernel) is

$$\omega(r,\theta,\varphi,\theta',\varphi') = \frac{1-r^2}{4\pi}\frac{1}{(1-2r[\cos\theta\cos\theta'+\sin\theta\sin\theta'\cos(\varphi-\varphi')]+r^2)^{3/2}}. \quad \text{(D5)}$$

Let us take the starting point (r,θ,φ) with $\theta = 0$ and $\varphi = 0$, i.e., the north pole. Because of the symmetry, the polar coordinate φ' of the first hitting point has a uniform distribution, from 0 to 2π. In turn, the azimuthal coordinate θ' has the density

$$p(\theta') = \frac{1-r^2}{2}\frac{\sin\theta'}{(1-2r\cos\theta'+r^2)^{3/2}}. \quad \text{(D6)}$$

The cumulative distribution function is

$$F(\theta) = \int_0^{\theta} d\theta' p(\theta') = \frac{1+r}{2r}\left(1-\frac{1-r}{\sqrt{1-2r\cos\theta+r^2}}\right). \quad \text{(D7)}$$

Inverting this relation, $F(\theta) = x$, one finds

$$\theta = \arccos\left(\frac{1+r^2}{2r} - \frac{(1-r^2)^2}{(2r)^3}\left[\frac{1+r}{2r}-x\right]^{-2}\right). \quad \text{(D8)}$$

One can thus generate the random azimuthal displacement θ with the harmonic measure density from a uniform number $x \in [0,1]$.

In summary, the random relocation by the bulk diffusion from the north pole $(r,\theta,\varphi) = (r,0,0)$ can be easily generated by using two uniformly distributed random numbers: $\varphi' \in [0,2\pi]$ and $x \in [0,1]$ (the latter yields θ').

When the starting point is different, one has to rotate the coordinates appropriately.

2. Simulation of displacements on the spherical surface in three dimensions

The following approach is inspired by [32]. The diffusion propagator on the sphere for the starting point at the north pole, $(\theta,\varphi) = (0,0)$, is well known:

$$\rho_t(\theta) = \sum_{n=0}^{\infty}\frac{2n+1}{4\pi R^2}e^{-Dn(n+1)t/R^2}P_n(\cos\theta), \quad \text{(D9)}$$

where R is the radius of the sphere, D the diffusion coefficient, and $P_n(z)$ the Legendre polynomials. The propagator does not depend on φ because of the symmetry. In practice, one can therefore generate the angle φ uniformly from $[0,2\pi]$, while the angle θ can be generated from the probability density

$$p_t(\theta) = 2\pi R^2 \sin\theta\rho_t(\theta) = \frac{1}{2}\sin\theta\sum_{n=0}^{\infty}(2n+1)e^{-Dn(n+1)t/R^2}P_n(\cos\theta). \quad \text{(D10)}$$

The orthogonality of Legendre polynomials implies the normalization of this density,

$$\int_0^{\pi} d\theta p_t(\theta) = 1. \quad \text{(D11)}$$

The cumulative distribution function $F_t(\theta)$ can be obtained by using the following relation for Legendre

polynomials:

$$(2n+1)P_n(x) = \frac{d}{dx}(P_{n+1}(x) - P_{n-1}(x)), \tag{D12}$$

from which

$$\begin{aligned} F_t(\theta) &\equiv \int_0^\theta d\theta' p_t(\theta') \\ &= \frac{1}{2}\left(1 + e^{-2c} - \sum_{n=1}^{\infty} P_n(\cos\theta)[e^{-c(n-1)n} \right. \\ &\quad \left. - e^{-c(n+1)(n+2)}]\right), \end{aligned} \tag{D13}$$

where $c = Dt/R^2$. As expected, this is a monotonously increasing function from 0 at $\theta = 0$ to 1 at $\theta = \pi$. The equation $F(\theta) = x$ can thus be numerically solved for any $x \in [0,1]$, in order to get $\theta = F^{-1}(x)$. This relation allows one to generate the angles θ from a uniformly distributed x.

In practice, for $c > 0.01$, the truncation with $N = 100$ is fair enough for an accurate computation of the function $F_t(\theta)$. The Legendre polynomials can be easily computed by the recursion formula,

$$(n+1)P_{n+1}(x) = (2n+1)xP_n(x) - nP_{n-1}(x), \tag{D14}$$

starting with $P_0 = 1$ and $P_1 = x$.

In the limit of very small c, one needs to get an alternative representation for the probability density $p_t(\theta)$ or the probability distribution $F_t(\theta)$.

a. Alternative representation

For simulation purposes, one often needs to set a small time step and to perform random displacements generated according to the propagator. In that case, Dt/R^2 is a small parameter so many terms are required in order to accurately approximate the above propagator. As pointed out in [32], the convergence of the series in Eq. (D10) is slow and the oscillatory character of the terms creates additional difficulties. As suggested in [32], one can use the Dirichlet-Mehler representation for Legendre polynomials,

$$P_n(\cos\theta) = \frac{\sqrt{2}}{\pi}\int_0^\pi \frac{\sin[(n+1/2)\alpha]d\alpha}{\sqrt{\cos\theta - \cos\alpha}}, \tag{D15}$$

and the Jacobi θ-function relation

$$\begin{aligned} &\sum_{n=0}^{\infty} e^{-cn(n+1)}\cos[(2n+1)x] \\ &\quad = \sqrt{\frac{\pi}{4c}}e^{c/4}\sum_{k=-\infty}^{\infty}(-1)^k e^{-(x+\pi k)^2/c}, \end{aligned} \tag{D16}$$

to get an alternative representation for the density

$$p_t(\theta) = \sin\theta\frac{\sqrt{2}e^{c/4}}{4\sqrt{\pi}c^{3/2}}\int_\theta^\pi \frac{g(\alpha)d\alpha}{\sqrt{\cos\theta - \cos\alpha}}, \tag{D17}$$

where $c = Dt/R^2$ and

$$g_c(\alpha) = \sum_{k=-\infty}^{\infty}(-1)^k(\alpha + 2\pi k)e^{-(\alpha+2\pi k)^2/(4c)}. \tag{D18}$$

When c is small enough, this sum can be truncated to few terms or even one term:

$$g_c^0(\alpha) = \alpha e^{-\alpha^2/(4c)}. \tag{D19}$$

Nevertheless, the computation of the integral in Eq. (D17) is still necessary. To overcome this difficulty, Carlsson *et al.* suggested to consider diffusion on a sphere in $\mathbb{R}^4$ (for which the computation is much easier) and then to project the resulting process on its equator, i.e., a sphere in $\mathbb{R}^3$ [32]. In spite of the elegance of this trick, it is worth mentioning that, in many practical cases, it is sufficient to compute the propagator $p_t(\theta)$ only once, for a given time step t. This computation can be easily and rapidly performed by a numerical integration in Eq. (D17). In what follows, we present the details of this computation.

To generate random angular displacement θ with a probability density $p_t(\theta)$, one needs to invert the cumulative distribution function

$$F_t(\theta) = 1 - \int_\theta^\pi d\theta' p_t(\theta'). \tag{D20}$$

For this purpose, we get

$$\begin{aligned} G_c(\theta) &\equiv \int_\theta^\pi d\theta' \sin\theta' \int_{\theta'}^\pi \frac{g_c(\alpha)d\alpha}{\sqrt{\cos\theta' - \cos\alpha}} \\ &= 2\int_\theta^\pi d\alpha g_c(\alpha)\sqrt{\cos\theta - \cos\alpha}, \end{aligned} \tag{D21}$$

so that

$$F_t(\theta) = 1 - \frac{\sqrt{2}e^{c/4}}{4\sqrt{\pi}c^{3/2}}G_c(\theta). \tag{D22}$$

These two approaches for computing $F_t(\theta)$ yield very accurate results. The direct summation in Eq. (D13) becomes more accurate for larger c, while the integral representation becomes more accurate for smaller c. They are therefore complementary to each other. In addition, the Gaussian approximation (D25) and its corrected version (D29) are also accurate.

b. Short-time approximation

For short times, the diffusion propagator can be approximated by the Gaussian propagator in two dimensions,

$$\rho_t(\theta) \approx \frac{1}{4\pi Dt}e^{-r^2/(4Dt)} = \frac{1}{4\pi R^2 c}e^{-\theta^2/(4c)}, \tag{D23}$$

from which

$$p_t(\theta) \approx \frac{1}{2c}\sin\theta e^{-\theta^2/(4c)} \approx \frac{1}{2c}\theta e^{-\theta^2/(4c)}, \tag{D24}$$

and

$$F_t(\theta) = \int_0^\theta d\theta' p_t(\theta') \approx 1 - e^{-\theta^2/(4c)}, \tag{D25}$$

from which the solution of the equation $F_t(\theta) = x$ reads as

$$\theta \approx \sqrt{-4c\ln(1-x)}, \tag{D26}$$

where x is a uniformly distributed random variable.

The same result can be obtained from the exact formula (D21). For short time, c is small so that large values of

α in the integral are negligible, while $g_c(\alpha)$ can be accurately approximated by $g_c^0(\alpha)$. Expanding $\cos\theta$ and $\cos\alpha$ into Taylor series and keeping the fourth order, one gets

$$\begin{aligned} G_c(\theta) &\approx 2\int_\theta^\pi d\alpha\alpha e^{-\alpha^2/(4c)}\sqrt{\frac{\alpha^2-\theta^2}{2}-\frac{\alpha^4-\theta^4}{24}} \\ &= \frac{1}{\sqrt{2}}\int_0^{\pi^2-\theta^2} dx e^{-(x+\theta^2)/(4c)}\sqrt{x}\sqrt{1-\frac{x+2\theta^2}{12}} \\ &\approx \frac{e^{-\theta^2/(4c)}}{\sqrt{2}}\left[(4c)^{3/2}(1-\theta^2/12)\int_0^{(\pi^2-\theta^2)/(4c)} dx e^{-x}x^{1/2}\right. \\ &\quad \left. -\frac{(4c)^{5/2}}{24}\int_0^{(\pi^2-\theta^2)/(4c)} dx e^{-x}x^{3/2}\right]. \end{aligned} \tag{D27}$$

For small c, the upper limit can be extended to infinity so that the integrals are simply $\Gamma(3/2)=\sqrt{\pi}/2$ and $\Gamma(5/2)=3\sqrt{\pi}/4$, yielding

$$G_c(\theta) \approx \frac{(4c)^{3/2}\sqrt{\pi}}{2\sqrt{2}}e^{-\theta^2/(4c)}[(1-\theta^2/12)-c/4], \tag{D28}$$

from which one gets the approximation

$$\begin{aligned} F_t(\theta) &\approx 1-e^{-\theta^2/(4c)+c/4}[(1-\theta^2/12)-c/4] \\ &\approx 1-e^{-\theta^2/(4c)}(1-\theta^2/12) \approx 1-e^{-\theta^2(1/(4c)+1/12)}. \end{aligned} \tag{D29}$$

Neglecting the correction term $1/12$ in comparison to the large $1/(4c)$, one retrieves the Gaussian approximation.

Inverting the equation $F_t(\theta)=x$, one gets

$$\theta \approx \sqrt{\frac{-\ln(1-x)}{1/(4c)+1/12}}, \tag{D30}$$

which allows one to generate the angle θ from a uniformly distributed random variable x. One can show that both approximations, Eq. (D26) and Eq. (D30), provide accurate results.

3. Rotations on the sphere

The above results were derived for the starting point at the north pole. They are of course applicable to any starting point by an appropriate rotation. For completeness, we provide the derivation of the underlying equations.

Let the starting point be at $A=(x,y,z)$, parametrized in spherical coordinates as

$$\begin{aligned} x &= \sin\theta\sin\varphi, \\ y &= \sin\theta\cos\varphi, \\ z &= \cos\theta \end{aligned} \tag{D31}$$

[in these coordinates, the north pole $(0,0,1)$ corresponds to $\theta=0$]. After a random move, the new point $B=(x',y',z')$ is parametrized as

$$\begin{aligned} x' &= \sin\theta'\sin\varphi', \\ y' &= \sin\theta'\cos\varphi', \\ z' &= \cos\theta'. \end{aligned} \tag{D32}$$

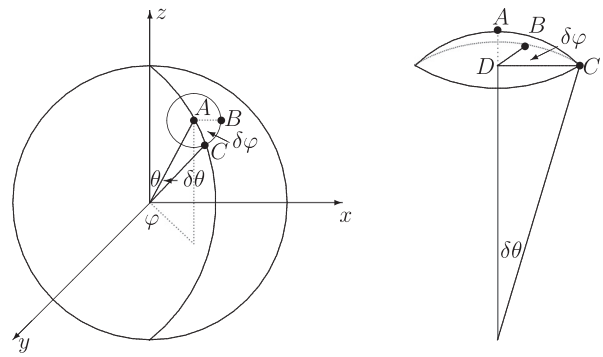

FIG. 8. Illustration for rotations on the unit sphere.

The new point belongs to a circle on the sphere which is centered at (x,y,z). Finally, we denote C a point on this circle which has the spherical coordinates $(\theta+\delta\theta,\varphi)$, where $\delta\theta$ is the random change of the angle θ (Fig. 8). First, we have

$$\begin{aligned} 1+1-2\cos\delta\theta &= |\mathrm{AB}|^2 = (x-x')^2+(y-y')^2 \\ &\quad +(z-z')^2 \\ &= 2-2(xx'+yy'+zz'), \end{aligned} \tag{D33}$$

from which

$$\cos\theta\cos\theta'+\sin\theta\sin\theta'\cos(\varphi-\varphi')=\cos\delta\theta. \tag{D34}$$

Second, we write

$$\begin{aligned} |\mathrm{BC}|^2 &= |\mathrm{DB}|^2+|\mathrm{DC}|^2-2|\mathrm{DB}||\mathrm{DC}|\cos\delta\varphi \\ &= 2|\mathrm{DB}|^2(1-\cos\delta\varphi) = 2\sin^2\delta\theta(1-\cos\delta\varphi). \end{aligned} \tag{D35}$$

On the other hand, we have

$$\begin{aligned} |\mathrm{BC}|^2 &= (\sin\theta'\sin\varphi'-\sin(\theta+\delta\theta)\sin\varphi)^2 \\ &\quad +(\sin\theta'\cos\varphi'-\sin(\theta+\delta\theta)\cos\varphi)^2 \\ &\quad +(\cos\theta'-\cos(\theta+\delta\theta))^2 \\ &= 2(1-\cos\theta'\cos(\theta+\delta\theta) \\ &\quad -\sin\theta'\sin(\theta+\delta\theta)\cos(\varphi-\varphi')), \end{aligned} \tag{D36}$$

from which

$$\begin{aligned} &\cos\theta'\cos(\theta+\delta\theta)-\sin\theta'\sin(\theta+\delta\theta)\cos(\varphi-\varphi') \\ &\quad = A \equiv 1-\sin^2\delta\theta(1-\cos\delta\varphi). \end{aligned} \tag{D37}$$

Two equations [Eqs. (D34) and (D37)] determine two unknown angles θ' and φ'. From the first equation, one gets

$$\cos(\varphi-\varphi') = \frac{\cos\delta\theta-\cos\theta\cos\theta'}{\sin\theta\sin\theta'}. \tag{D38}$$

Substituting this expression into the second equation, one obtains after some transformations

$$\cos\theta' = \cos(\theta+\delta\theta)+\sin(\theta)\sin(\delta\theta)(1-\cos\delta\varphi). \tag{D39}$$

If the angular change $\delta\theta$ is small, the new angle is simply $\theta'=\theta+\delta\theta\cos\delta\varphi$ (in the first order of $\delta\theta$). However, this is

insufficient for computing the correction to φ' which needs the second order. For $\delta\theta \ll \theta$, one gets

$$\theta' = \theta + \delta\theta\cos\delta\varphi + \frac{(\delta\theta)^2}{2}\frac{\cos\theta}{\sin\theta}\sin^2\delta\varphi + O(\delta\theta^3),$$
$$\varphi' = \varphi + \delta\theta\frac{\sin\delta\varphi}{\sin\theta} + O(\delta\theta^2). \tag{D40}$$

It is expected that the correction to φ diverges as $\theta \to 0$ because the angle φ is not defined at $\theta = 0$.

4. Discretization of the sphere

The final point is a discretization of the sphere. In practice, one needs to discretize both angles, $\theta \in (0,\pi)$ and $\varphi \in (0,2\pi)$. The discretization of φ is naturally uniform: $\varphi_j = j\sigma_\varphi$, $j = 0,\ldots,N_\varphi - 1$, with $\sigma_\varphi = 2\pi/N_\varphi$.

Let us assume that the angle θ is discretized by a set $\{\theta_k\}$, $k = 0,\ldots,N_\theta - 1$. One can easily compute the surface area for each "cell" of such discretization. In fact, the surface area of a spherical cap of angle θ is simply $S(\theta) = 2\pi(1-\cos\theta)$ so that

$$s_{jk} = \frac{\sigma_\varphi}{2\pi}[S(\theta_{k+1}) - S(\theta_k)] = \sigma_\varphi(\cos\theta_k - \cos\theta_{k+1}), \tag{D41}$$

independently of the index j of the angle φ. If we require that all s_{jk} are equal to some s_0, this naturally leads to the "optimal" choice of the discretization points θ_k:

$$\cos\theta_{k+1} = \cos\theta_k - \frac{s_0}{\sigma_\varphi}, \tag{D42}$$

starting with $\theta_0 = 0$. In particular, setting s_0/σ_φ determines the number N_θ of "layers" in θ in such a way that $\theta_{N_\theta} = \pi$: $N_\theta = 2\sigma_\varphi/s_0$. In other words, one has to ensure that $\cos\theta_k$ are uniformly sampled on the interval $(-1,1)$.

Note that if the uniform distribution of θ_k was used, $\theta_k = k\sigma_\theta$, one would have

$$\begin{aligned} s_{jk} &= \sigma_\varphi[\cos(k\sigma_\theta) - \cos((k+1)\sigma_\theta)] \\ &= \sigma_\varphi[\cos(k\sigma_\theta)(1-\cos(\sigma_\theta)) + \sin(k\sigma_\theta)\sin(\sigma_\theta)] \\ &\approx \sigma_\varphi\sigma_\theta\sin(k\sigma_\theta). \end{aligned} \tag{D43}$$

5. The algorithm

The Monte Carlo algorithm consists in the following steps.

(1) Initialize the physical parameters (R, D_1, D_2, a, ϵ, λ) and the numerical parameters (number of walks M, discretization time step δ). The time step δ determines the spatial discretization $\sigma = \sqrt{4D_1\delta}$.

(2) Allocate memory for the array of explored territory counters on the discretized spherical surface.

(3) Choose the initial position (θ_0,φ_0) (either fixed, or uniformly distributed over the sphere).

(4) Check that the particle did not reach the target (i.e., $\theta > \epsilon$). If reached, one moves to step 3 for a new walk.

(5) Update the array of explored territory counters by the present position.

(6) Generate a uniform random number x and check the condition $x < e^{-\lambda\delta}$. If true, then the particle remains on the surface; otherwise, a desorption event occurs.

(7) Generate the uniform angle $\delta\varphi \in (0,2\pi)$ and the angle $\delta\theta$ according to either Eq. (D30) for surface displacement or Eq. (D8) for bulk displacement.

(8) Update the current position (θ_k,φ_k).

(9) Return to step 4.

[1] R. D. Astumian and P. B. Chock, J. Phys. Chem. **89**, 3477 (1985).
[2] G. Adam and M. Delbrück, *Reduction of Dimensionality in Biological Diffusion Processes* (Freeman, San Francisco, CA, 1968).
[3] H. Sano and M. Tachiya, J. Chem. Phys. **75**, 2870 (1981).
[4] Z. Schuss, A. Singer, and D. Holcman, Proc. Natl. Acad. Sci. USA **104**, 16098 (2007).
[5] G. C. Bond, *Heterogeneous Catalysis: Principles and Applications* (Clarendon, Oxford, 1987).
[6] R. Walder, N. Nelson, and D. K. Schwartz, Phys. Rev. Lett. **107**, 156102 (2011).
[7] M. J. Skaug, J. Mabry, and D. K. Schwartz, Phys. Rev. Lett. **110**, 256101 (2013).
[8] O. Benichou, C. Loverdo, M. Moreau, and R. Voituriez, Phys. Chem. Chem. Phys. **10**, 7059 (2008).
[9] A. V. Chechkin, I. M. Zaid, M. A. Lomholt, I. M. Sokolov, and R. Metzler, Phys. Rev. E **79**, 040105(R) (2009).
[10] G. Oshanin, M. Tamm, and O. Vasilyev, J. Chem. Phys. **132**, 235101 (2010).
[11] O. Bénichou, D. Grebenkov, P. Levitz, C. Loverdo, and R. Voituriez, Phys. Rev. Lett. **105**, 150606 (2010).
[12] O. Bénichou, D. Grebenkov, P. Levitz, C. Loverdo, and R. Voituriez, J. Stat. Phys. **142**, 657 (2011).
[13] A. V. Chechkin, I. M. Zaid, M. A. Lomholt, I. M. Sokolov, and R. Metzler, J. Chem. Phys. **134**, 204116 (2011).
[14] F. Rojo and C. E. Budde, Phys. Rev. E **84**, 021117 (2011).
[15] F. Rojo, H. S. Wio, and C. E. Budde, Phys. Rev. E **86**, 031105 (2012).
[16] F. Rojo, C. E. Budde, Jr., H. S. Wio, and C. E. Budde, Phys. Rev. E **87**, 012115 (2013).
[17] A. M. Berezhkovskii and A. V. Barzykin, J. Chem. Phys. **136**, 054115 (2012).
[18] G. Weiss, *Aspects and Applications of the Random Walk* (North-Holland, Amsterdam, 1994).
[19] B. Hughes, *Random Walks and Random Environments* (Oxford University Press, New York, 1995).
[20] H. Larralde, P. Trunfio, S. Havlin, H. E. Stanley, and G. H. Weiss, Nature (London) **355**, 423 (1992).
[21] A. Blumen, J. Klafter, and G. Zumofen, in *Optical Spectroscopy of Glasses*, edited by I. Zschokke (Reidel, Dordrecht, 1986).
[22] D. Ben-Avraham and S. Havlin, *Diffusion and Reactions in Fractals and Disordered Systems* (Cambridge University Press, Cambridge, UK, 2000).
[23] T. Calandre, O. Bénichou, D. S. Grebenkov, and R. Voituriez, Phys. Rev. E **85**, 051111 (2012).
[24] J. F. Rupprecht, O. Bénichou, D. S. Grebenkov, and R. Voituriez, Phys. Rev. E **86**, 041135 (2012).

[25] J. F. Rupprecht, O. Bénichou, D. Grebenkov, and R. Voituriez, J. Stat. Phys. **147**, 891 (2012).

[26] A. M. Berezhkovskii, Y. A. Makhnovskii, and R. A. Suris, J. Stat. Phys. **57**, 333 (1989).

[27] C.W. Gardiner, *Handbook of Stochastic Methods for Physics, Chemistry and Natural Sciences* (Springer, Berlin, 2004).

[28] S. Redner, *A Guide to First-Passage Processes* (Cambridge University Press, Cambridge, U.K., 2001).

[29] S. Condamin, O. Bénichou, V. Tejedor, R. Voituriez, and J. Klafter, Nature (London) **450**, 77 (2007); S. Condamin, O. Benichou, and M. Moreau, Phys. Rev. E **75**, 021111 (2007); O. Benichou, B. Meyer, V. Tejedor, and R. Voituriez, Phys. Rev. Lett. **101**, 130601 (2008); S. Condamin, V. Tejedor, R. Voituriez, O. Benichou, and J. Klafter, Proc. Natl. Acad. Sci. USA **105**, 5675 (2008); C. Chevalier, O. Bénichou, B. Meyer, and R. Voituriez, J. Phys. A: Math. Theor. **44**, 025002 (2011).

[30] O. Bénichou, M. Coppey, M. Moreau, P. H. Suet, and R. Voituriez, J. Phys.: Condens. Matter **17**, S4275 (2005).

[31] G. Barton, *Elements of Green Functions and Propagation: Potentials, Diffusion and Waves* (Oxford University Press, New York, 1989).

[32] T. Carlsson, T. Ekholm, and C. Elvingson, J. Phys. A: Math. Theor. **43**, 505001 (2010).